




Original Article



IL-33 Downregulates Hepatic Carboxylesterase 1 in Acute Liver Injury via Macrophage-Derived Exosomal miR-27b-3p

Ping Gao^{1#}, Min Li^{2#}, Jingli Lu³, Daochun Xiang⁴, Ximin Wang², Yanjiao Xu², Yue Zu², Xinlei Guan⁵, Guodong Li² and Chengliang Zhang^{2*} 

¹Wuhan Children's Hospital, Tongji Medical College, Huazhong University of Science and Technology, Wuhan, Hubei, China; ²Tongji Hospital Affiliated with Tongji Medical College, Huazhong University of Science and Technology, Wuhan, Hubei, China; ³The First Affiliated Hospital of Zhengzhou University, Zhengzhou, China; ⁴The Central Hospital of Wuhan, Tongji Medical College, Huazhong University of Science and Technology, Wuhan, Hubei, China; ⁵Wuhan Forth Hospital, Wuhan, Hubei, China

Received: 6 December 2022 | Revised: 19 January 2023 | Accepted: 23 February 2023 | Published online: 16 March 2023

Abstract

Background and Aims: We previously reported that carboxylesterase 1 (CES1) expression was suppressed following liver injury. The study aimed to explore the role of interleukin (IL)-33 in liver injury and examine the mechanism by which IL-33 regulates CES1. **Methods:** IL-33 and CES1 levels were determined in the livers of patients and lipopolysaccharide (LPS)-, acetaminophen (APAP)-treated mice. We constructed IL-33 and ST2 knockout (KO) mice. ST2-enriched immune cells in livers were screened to identify the responsible cells. Macrophage-derived exosome (MDE) activity was tested by adding exosome inhibitors. Micro-RNAs (miRs) were extracted from control and IL-33-stimulated MDEs (IL-33-MDEs) and subjected to miR sequencing (miR-Seq). Candidate miR was tested *in vitro* and *in vivo* and its binding of a target gene was assessed by luciferase reporter assays. Lentivirus-vector cellular transfection and transcript silencing were used to examine pathways mediating IL-33 suppression of miR-27b-3p. **Results:** Patient liver IL-33 and CES1 expression levels were inversely correlated. CES1 downregulation in liver injury was rescued in both IL-33-deficient and ST2 KO mice. Macrophages were shown to be responsible for IL-33 effects. IL-33-MDEs reduced CES1 levels in hepatocytes. Exosomal miR-Seq and qRT-PCR demonstrated increased miR-27b-3p levels in IL-33-MDEs; miR-27b-3p was implicated in *Nrf2* targeting. IL-33 inhibition of miR-27b-3p was found to be GATA3-dependent. **Conclusions:** IL-33-ST2-GATA3 pathway signaling increases miR-27b-3p content in MDEs, which upon being internalized by hepatocytes reduce CES1 expression by inhibiting *Nrf2*. The elucidation of this mechanism

in this study contributes to a better understanding of CES1 dysregulation in liver injury.

Citation of this article: Gao P, Li M, Lu J, Xiang D, Wang X, Xu Y, et al. IL-33 Downregulates Hepatic Carboxylesterase 1 in Acute Liver Injury via Macrophage-Derived Exosomal miR-27b-3p. J Clin Transl Hepatol 2023. doi: 10.14218/JCTH.2022.00144.

Introduction

Carboxylesterases (CESs, EC.3.1.1.1) are serine hydrolase superfamily proteins that hydrolyze ester, thioester, amide, and carbamate linkages, thus playing critical roles in both endobiotic metabolism and inactivation as well as xenobiotic detoxification.¹ There are three CES human subtypes, among which CES1 is highly expressed in the liver. CES1 serves as an important mediator of drug metabolism, activation, and detoxification, and accounts for 80–95% of total hepatic hydrolytic activity. Hence, the function and expression of CES1 affect the clinical efficacy and outcomes of various drugs that act as CES1 substrates.² Moreover, CES1 acts on a wide range of physiological and cellular processes, including fatty acid metabolism and cholesterol hydrolysis. Consequently, CES dysfunction can lead to atherosclerosis, hypercholesterolemia, and obesity.^{3–5} Understanding CES1 expression and regulatory mechanisms in specific physiological states is, therefore, of great significance for clinical diagnosis and treatment.

Drug-metabolizing enzymes are numerous and abundant in the liver, making the liver a primary site for the metabolism and clearance of a variety of molecules, including drugs and xenobiotics as well as endogenous compounds.⁶ As a consequence, the liver is vulnerable to damage from a variety of factors, including drugs, alcohol, and infections. Liver injury can alter the expression and activity of drug-metabolizing enzymes.^{7,8} Our previous work has shown that CES1 expression and metabolic activities are suppressed in liver-injured rats.⁷ The mechanism underlying CES1 downregulation in liver injury remains unknown.

Inflammation has long been known to contribute to liver

Keywords: IL-33; Carboxylesterase 1; miR-27b-3p; Liver injury.

Abbreviations: ALF, acute liver failure; ALT, alanine aminotransferase; APAP, acetaminophen; AST, aspartate aminotransferase; CES1, carboxylesterase 1; FBS, fetal bovine serum; HCC, hepatocellular carcinoma; IL, interleukin; KO, knockout; LPS, lipopolysaccharide; MDE, macrophage-derived exosome; miR, micro-RNA; MyD88, myeloid differentiation primary response 88; Nrf2, nuclear factor erythroid 2-related factor 2; PBS, phosphate buffered saline; SD, standard deviation; UTR, untranslated region; WT, wild type.

*Contributed equally to this manuscript.

*Correspondence to: Chengliang Zhang, Tongji Hospital Affiliated with Tongji Medical College, Huazhong University of Science and Technology, Wuhan, Hubei 430030, China. ORCID: <https://orcid.org/0000-0001-9429-4764>. Tel: +86-27-83663519, Fax: +86-27-83663643, E-mail: clzhang@tjh.tjmu.edu.cn

injury,⁹ and the expression of hepatic enzymes is regulated by inflammatory cytokines, including interleukins (ILs).¹⁰ For example, data from our previous study showed that IL-6 inhibits CES expression.¹¹ Many studies suggested that IL-1 family proteins could regulate the expression of various cytochrome P450 enzymes.^{10,12} IL-33, an IL-1 family member, is constitutively expressed in many human tissues. Both liver sinusoidal endothelial cells and liver macrophages express high levels of IL-33.¹³ Under steady-state conditions, IL-33 is stored in the cell nucleus. Upon cellular damage, IL-33 is released from severely injured or necrotic cells into the extracellular space, where it can bind the orphan receptor ST2 (also known as IL-1 receptor-like 1) cell surface receptor complex, and thereby activate multiple intracellular signaling pathways. As a recognized alarmin that is released in response to tissue injury, IL-33 has been implicated in several liver diseases, including alcoholic hepatitis,¹⁴ viral hepatitis,¹⁵ ischemia/reperfusion liver injury,¹⁶ and acetaminophen (APAP)-induced liver injury.¹³ Although the importance of IL-33 in liver diseases is well established, IL-33 effects on hepatic enzymes and the underlying mechanisms of such effects have yet to be clarified.

In this study, we identified IL-33 as an important suppressor of CES1 in liver injury, specifically in a ST2 dependent manner. Furthermore, we found that IL-33 increased miR-27b-3p content in macrophage-derived exosomes through GATA3. These exosomes were then transferred to hepatocytes and restrained the expression of CES1 by inhibiting Nrf2 which was identified as the target gene of miR-27b-3p. Altogether, our data provide evidence of a previously unknown pathway by which IL-33 regulates CES1.

Methods

Patient specimens

A total of 14 liver tissue samples were collected, including samples collected from seven patients with acute liver failure (ALF) and seven patients with hepatocellular carcinoma (HCC) at the Tongji Hospital, Tongji Medical College, Huazhong University of Science and Technology (HUST). Patients with HCC showed normal liver functions and lacked any notable inflammation. After liver tissue was isolated, it was fixed with 10% formalin, and sent to the pathology department for paraffin embedding and sectioning for immunohistochemistry and immunofluorescence studies. All experimental procedures were performed in accordance with the Declaration of Helsinki of the World Medical Association and were approved by the Medical Ethics Committee of Tongji Hospital (no: TJ-IRB20210961).

Animal experiments

Eight-week-old male C57BL/6 mice were obtained from Gempharmatech (Nanjing, China). IL-33 KO mice and ST2 deficient mice were kindly donated by Dr. Fang Zheng (Department of Immunology, Tongji Medical College, HUST), and Shulaibao Biotechnology carried out mouse propagation and identification. Mice were housed at 21–23°C with a 12 h light/dark cycle. Food and water were available ad libitum. LPS¹⁷ and APAP-induced acute liver injury models in mice were generated as previously described.¹⁸ The mice were sacrificed 16 h after injury induction, and their livers and blood were harvested. Serum was separated by centrifugation at 4,000 rpm for 10 min and stored at –20°C for further use. Livers were fixed with 10% neutral buffered formalin or preserved at –80°C for further use. All mice were bred and maintained under specific pathogen-free conditions and

studied in compliance with the Animal Care and Use Committee guidelines of Tongji Hospital, Tongji Medical College, HUST.

CES1 activity determination

Thawed livers were homogenized in buffer made of 50 mM Tris-HCl, 150 mM KCl and 2 mM ethylenediaminetetraacetic acid. The homogenate was centrifuged at 9,000 *g* for 30 min, and the supernatant fraction was further centrifuged at 100,000 *g* for 1 h.⁷ The hepatic microsomal pellet was resuspended in phosphate buffer containing 20% glycerol and stored at –80°C until further use. CES1 activities were measured in reaction mixtures containing 0.1 mg/mL of microsomal protein with 10 mM phosphate-buffered saline solution (pH=7.4) to make a total volume of 200 μ L. After 5 min preincubation at 37°C, the reaction was initiated by adding 5 μ L clopidogrel, followed by incubation at 37 °C for 60 min. The reaction was terminated by adding ice-cold tert-butyl methyl ether and n-hexane (3:1, V/V), and 50 μ L of the internal standard ticlopidine were then added. The mixture was vortexed for 5 min after centrifugation at 4,000 *g* for 5 min; the supernatant was evaporated to dryness, and the residue was dissolved in 0.1 mL of a mobile phase for high-performance liquid chromatography-tandem mass spectrometry (LC-MS/MS) analysis.

Histology

Liver samples were fixed in 4% paraformaldehyde and then paraffin-embedded using a standard method. Fixed tissue samples were sectioned and stained with hematoxylin and eosin (H&E). Pictures were taken using an Olympus BX-53 microscope. For immunohistochemical labeling, after preincubation with 3% hydrogen peroxide and blocking with 2% bovine serum albumin (Amresco, Solon, OH, USA), sections were stained with anti-IL-33 (WC3234729; Invitrogen Life Technologies, Carlsbad, CA, USA), anti-CES1 (ERP1375Y; Abcam, Cambridge, UK), or anti-F4/80 antibody (B281627; Biolegend, San Diego, CA, USA) overnight at 4 °C. After washing, sections were incubated with respective secondary antibodies. For immunofluorescent labeling, paraffin-embedded human liver tissue sections were deparaffinized, rehydrated, and antigen was retrieved by Tris- ethylenediamine-tetraacetic acid buffer for 95°C for 30 min. Then, the sections were incubated with anti-IL-33 antibody (WC3234729; Invitrogen) at 4°C overnight, secondary antibody the next day, and the mounted with 4',6-diamidino-2-phenylindole. Positive staining was visualized using an Olympus BX-51 fluorescence microscope. The total stained area was analyzed by ImageJ (NIH, Bethesda, MD, USA).

Biochemical assays

Serum samples were processed in accordance with manufacturer's instructions of the commercial kits (Jiancheng Bioengineering Institute, Nanjing, China), and then the activities of alanine aminotransferase (ALT) and aspartate aminotransferase (AST) were quantified on a multifunction microplate reader (ELx800; Bio-TEK, Winooski, VT, USA).

Quantitative reverse transcriptase (qRT)-PCR

TRIzol reagent (Invitrogen) was used to extract total RNA from liver tissues. To prevent genomic DNA contamination, the extracts were treated with DNase I (Takara, Shiga, Japan). First-strand cDNA was synthesized from 1 μ g of each RNA on PCR beads with an oligo (dT) primer (Amersham Bioscience, Buckinghamshire, UK). Gene expression was detected via PCR (40 cycles of 95°C for 15 s, 58 °C for 15 s, and 72°C for

45 s) with the following primers: glyceraldehyde-phosphate dehydrogenase (GAPDH), forward 5'-CGTT GACATCCGTAAA-GACCT-C-3' and reverse 5'-TAGGAGCCAGGGCAGTAA TCT-3'; CES1, forward 5'-AGGTCTGGGGAAGTATGCC-3' and reverse 5'-TGCATCTTGGGAGCACATAGG-3'; Nrf2, forward 5'-CTCGCTGGAAAAAGAA GTG-3' and reverse 5'-CCGTCCAG-GAGTTCAGAGG-3'. mRNA levels were normalized relative to GAPDH.

Western blotting

Equal quantities of liver tissue and cell extracted proteins were separated by 10% sodium dodecyl-sulfate polyacrylamide gel electrophoresis (SDS-PAGE) and then transferred to polyvinylidene fluoride membranes (Hybond, Escondido, CA, USA). The protein-loaded membranes were blocked with defatted milk (5%) at room temperature for 2 h, incubated overnight with primary antibodies (Supplementary Table 1) at 4°C, and then incubated with secondary antibodies for 2 h at room temperature. Enhanced chemiluminescence (Pierce Biotechnology, Waltham, MA, USA) was used to visualize the blots. The protein amount was 20 µg in each sample. The loading control was β-actin. All assays were completed at least three times.

Primary hepatocyte isolation and culture

Primary mouse hepatocytes were isolated as previously reported.¹⁹ In brief, livers were perfused and digested with calcium-free solution and collagenase, and then filtered through 100 µm cell strainer. Hepatocytes were collected by centrifugation of the filtration liquid at 50 g, 4°C for 5 m, and plated in collagen-coated plates with Dulbecco's modified Eagle medium (DMEM) plus 10% fetal bovine serum (FBS). Hepatocytes were seeded in at a density of 250,000 cells/plate. Four hours later, the plates were washed to remove nonadhering cells. Cells were cultured at 37°C in a 5% CO₂ incubator and maintained in DMEM supplemented with 10% FBS and 1% penicillin-streptomycin.

Cell line cultures

Both human hepatic progenitor cell line (HepaRG) cells and murine macrophage cell line (RAW 264.7) cells (Otto Biotech, Wuhan, China; National Collection of Authenticated Cell Culture, Shanghai, China) were cultured at 37°C in 5% CO₂ and maintained in DMEM supplemented with 10% FBS and 1% penicillin-streptomycin. To determine whether exosomes were involved in macrophage-induced downregulation of CES1, 10 µM GW4869 (Sigma-Aldrich, St Louis, MO, USA) was used to reduce the release of the exosomes from macrophages. For exosome processing, mouse primary hepatocytes or HepaRG cells were cultured with exosome-free serum and supplemented with 100 µg/mL phosphate buffered saline (PBS) or MDEs. The cells were collected after 24 h in culture.

Flow cytometry

Livers of mice treated with LPS, or vehicle were perfused, digested and filtered as stated above. And then hepatic nonparenchymal cells were collected through centrifuging at 500 g, 4°C for 5 m. Cell suspensions were incubated with Fc-blocker (2.4 G2; BD PharMingen, Franklin Lakes, NJ, USA) and Zombie aqua dye (Biolegend) for 10 m. The cells were incubated at 4°C in the dark for 30 m with the following antibodies: anti-CD3 (#38527; CST, Danvers, MA, USA), anti-Ly6G (ab238132; Abcam), anti-F4/80 (sc-52664; Santa Cruz Biotechnology, Dallas, TX, USA). Flow cytometry was performed in a FACSCalibur machine (BD Biosciences, Waltham, MA, USA).

Macrophage depletion

The purchased clodronate liposomes contain 5 mg/mL clodronate in the suspension (Formumax, Sunnyvale, CA, USA). Liver monocytes/macrophages were depleted transiently with a 200 µL aliquot of clodronate liposomes per mouse. The liposomes were injected intravenously 24 h before LPS administration. Mice in the control group received a corresponding number of PBS-filled liposomes. Macrophage depletion efficiency was assessed by flow cytometry.

Exosome isolation and characterization

Exosomes were isolated and characterized as previously reported.²⁰ In brief, RAW264.7 macrophages (70–80% confluence) were cultured at 37°C in a 5% CO₂ incubator, with or without 20 ng/mL IL-33 in high glucose DMEM (Gibco BRL of Thermo Fisher Scientific, Waltham, MA, USA) with 10% exosome-depleted FBS for 24 h. Subsequently, samples of media were transferred to 50 mL tubes and centrifuged at 300 g for 10 m. The supernatant was collected and centrifuged on low speed (2,000 g for 10 m) to discard cell debris. The supernatant was then centrifuged at 10,000 g for 30 m followed by ultracentrifugation for 70 m at 100,000 g (Sorvall WX 100+; Thermo Fisher Scientific). The pelleted exosomes were washed twice with ample PBS and recentrifuged at 100,000 g for 70 m. Nanoparticle tracing analysis to characterize exosome concentrations was performed by Zetaview (Particle Metrix, Meerbusch, Germany), and exosome morphology was observed with transmission electron microscopy (Hitachi, Tokyo, Japan).

Labeling and cellular uptake of exosomes

Following membrane labeling with PKH67 as the manufacturer's instruction (Invitrogen), the labeled exosomes were washed in PBS and centrifuged 100,000 g for 20 min at 4°C. The purified exosomes were re-suspended in serum-free medium. Hepatocytes were then seeded into a single layer in glass bottom dishes (Cellvis, Mountain View, CA, USA), co-cultured with PKH67-labeled exosomes (30, 60, or 120 min), washed with PBS three times, and fixed in 4% paraformaldehyde. The fixed hepatocytes were stained with DiI (Invitrogen), washed with PBS, and imaged by confocal microscopy (TCS SP8; Leica, Wetzlar, Germany).

miR-Seq and differential expression analysis

Exosome miR-Seq analysis was conducted with control and IL-33-stimulated MDEs by Siwega (Wuhan, China). The criteria for recognizing differentially expressed miRs were: $|\log_2(\text{fold change})| > 1$ and $p < 0.05$. To validate miRs identified through RNA sequencing total RNA was extracted from cells with RNAiso Plus reagent (Takara) according to the manufacturer's instructions. The extracted miRs were purified and subjected to real-time quantitative reverse transcription (qRT)-PCR as described elsewhere.²⁰ Reverse transcription (miR reverse transcription kit; Takara) and real-time SYBR Green (Applied Biosystems Plus PCR System; Applied Biosystems, Waltham, MA, USA) fluorescence quantitative PCR were performed. The miR primer sets were purchased from Tsingke Biotechnology (Beijing, China). Expression of intracellular miR was normalized to that of U6 (internal reference gene); expression of exosomal miR was normalized to cel-miR-39 (internal reference miR).

miR transfection

Lipofectamine 2000 (Invitrogen, Waltham, MA, USA) transfection protocols were performed on miR-27b-3p mimics, miR-27b-3p inhibitors, and their negative controls according

to the manufacturer's directions. Hepatocytes were cultured to 70% confluence. A transfection reagent was mixed with miR-27b-3p mimics, miR-27b-3p inhibitor, and their negative controls. Each miR product was then added to a cell culture (final concentration of 50–100 nmol/L). qRT-PCR was used to determine transfection efficiency.

Luciferase reporter assay

Cells were cotransfected with wild-type (WT) or mutant 3'-untranslated region (UTR) of *Nrf2* and miR-27b-3p mimics or miR-Control with Lipofectamine 3000 (Invitrogen) luciferase vectors. Luciferase activity was measured 48 h after transfection with a dual-luciferase reporter assay system (Beyotime, Jiangsu, China).

Cell transfection

HepaRG cells were transfected with lentivirus vectors encoding *Nrf2* (hU6-*Nrf2*-Ubiquitin-EGFP-IRES-puromycin; Genechem Company, Shanghai, China). RAW 264.7 macrophages were transfected into lentivirus vectors encoding *Gata3* (hU6-*GATA3*-Ubiquitin-EGFP-IRES-puromycin; Genechem Company). Empty plasmids were transfected into HepaRG cells and macrophages as controls, respectively. Transfection efficiency was determined by confocal laser scanning microscopy on a LSM 800 microscope (Zeiss, Oberkochen, Germany); over 80% fluorescence-positive cells were considered acceptable efficiency. Silencing (si)RNA oligonucleotides for *Gata3* and a noncoding siRNA with no biological effects were procured from Genechem, and siRNA (50 nM) transfection was performed for 24 h or 48 h according to the manufacturer's protocol. *Gata3* knockdown efficiency was determined by qRT-PCR and western blot assays.

Prediction of miR targets

To identify likely targets of miRs of interest, computational analysis was performed with TargetScan, miRDB, RNA22 and miRTarBase databases.

Statistical analysis

All data are shown as means \pm standard deviations (SDs). Linear associations between IL-33 and CES1 were determined by calculating Pearson's correlation coefficient. Variance among multiple groups was assessed with one-way analysis of variance and least significant difference *post-hoc* analyses. Student's *t*-tests were used to detect differences between paired groups. A *p* value of <0.05 was considered statistically significant. All authors had access to the study data and had reviewed and approved the final manuscript.

Results

IL-33 downregulates hepatic CES1 in injured liver

Examination of hepatic IL-33 levels with immunofluorescence showed that, compared to the HCC group, IL-33 expression was increased in ALF patients (Fig. 1A). CES1 was significantly suppressed in ALF patients compared with levels seen in HCC patients (Fig. 1A). Regression analysis showed a negative correlation between IL-33 and CES1 expression levels in livers ($p < 0.001$) (Fig. 1B). IL-33 protein levels were also found to be higher in LPS-treated mice than in control mice (Fig. 1C, D). Similarly, CES1 mRNA levels, protein levels, and metabolic activity were significantly decreased in LPS-treated mice (Fig. 1C–F). A similar expression pattern of IL-33 and CES1 was observed in APAP-treated mice (Supplementary Fig. 1A–D).

CES1 downregulation in LPS-induced liver injury was abrogated in IL-33 KO mice (Fig. 1G, H, and Supplementary Fig. 1E, F). Restoration of CES1 was also observed in ST2 KO mice (Fig. 1G, H). Likewise, CES1 expression was found to be rescued by removal of IL-33 or ST2 in APAP-treated mice (Supplementary Fig. 1G, H). These data provide compelling evidence that IL-33–ST2 signaling is essential for CES1 downregulation in liver injury. The extent of liver damage caused by LPS and APAP was attenuated in both the IL-33 KO and ST2 KO mice, as evidenced by serum ALT, serum AST, and H&E staining of liver tissue (Supplementary Fig. 1I–L).

Macrophages play a bridging role in IL-33 induced downregulation of CES1

To reveal the potential mechanism of IL-33 on CES1, mouse primary hepatocytes, the main hepatic source of CES1,²¹ were treated with serial concentrations of IL-33 (5, 10 and 20 ng/mL). Unexpectedly, IL-33 did not alter CES1 mRNA or protein levels in primary mouse hepatocytes compared to the control group (Fig. 2A, B). It has been demonstrated that immune cells constitute major cellular targets of IL-33 *in vivo*.²² Therefore, we analyzed the change of common hepatic immune cell subsets related to liver injury, including macrophages, T cells, and neutrophils.²³ Flow cytometry analysis of these immune cells with corresponding specific markers (F4/80, CD3 and Ly6G) showed that, after LPS stimulation, T cells and neutrophils were slightly increased ($p > 0.05$) (Fig. 2C, D), while macrophage infiltration was dramatically increased in liver-injured mice ($p < 0.01$, Fig. 2C, D). Subsequently, immunohistochemistry analysis revealed that F4/80⁺ cells did significantly increase in the livers of LPS-treated mice (Fig. 2E). Compared with mice receiving blank vehicle, macrophage-depleted mice had greater levels of CES1 in the liver after LPS treatment (Fig. 2F, G). Altogether, these data suggest that macrophages are involved in IL-33 induced downregulation of CES1 in response to liver injury.

MDEs mediate IL-33 influence on CES1

Exosomes were recently considered a novel way of cell-to-cell communication, therefore, we isolated and investigated whether macrophage-derived exosomes were involved in the downregulation of CES1 by IL-33. Quantitative nanoparticle tracking analysis of isolated MDEs indicated that control (Con-MDEs) and IL-33-stimulated MDEs (IL-33-MDEs) were of similar size and were present at similar particle concentrations (Fig. 3A). TEM showed that both MDE groups had a typical round or cup-shaped morphology (Fig. 3B). Western blot analysis demonstrated the presence of exosomal protein, TSG101, CD9, and Annexin A1, but not the presence of the endoplasmic reticulum marker Calnexin in MDEs (Fig. 3C). Confocal microscopy of fluorescent PKH67-labeled MDEs that had been co-cultured with primary hepatocytes for 24 h demonstrated the MDE uptake by hepatocytes (Fig. 3D).

Hepatocytes treated with IL-33-MDEs had reduced CES1 mRNA and protein levels compared to hepatocytes treated with Con-MDEs or PBS (Fig. 3E, F). The addition of GW4869, a neutral sphingomyelinase inhibitor that prevents exosome release from macrophages, reversed IL-33's suppressive effects on CES1 expression (Fig. 3G, H), indicating that the IL-33 effects were exosome dependent.

miR-27b-3p transferred by MDEs downregulates CES1

To investigate whether miRs, as exosome cargo, participate in IL-33 inhibition of CES1, we conducted exosomal miR sequencing on Con-MDEs and IL-33-MDEs. Among the miRs

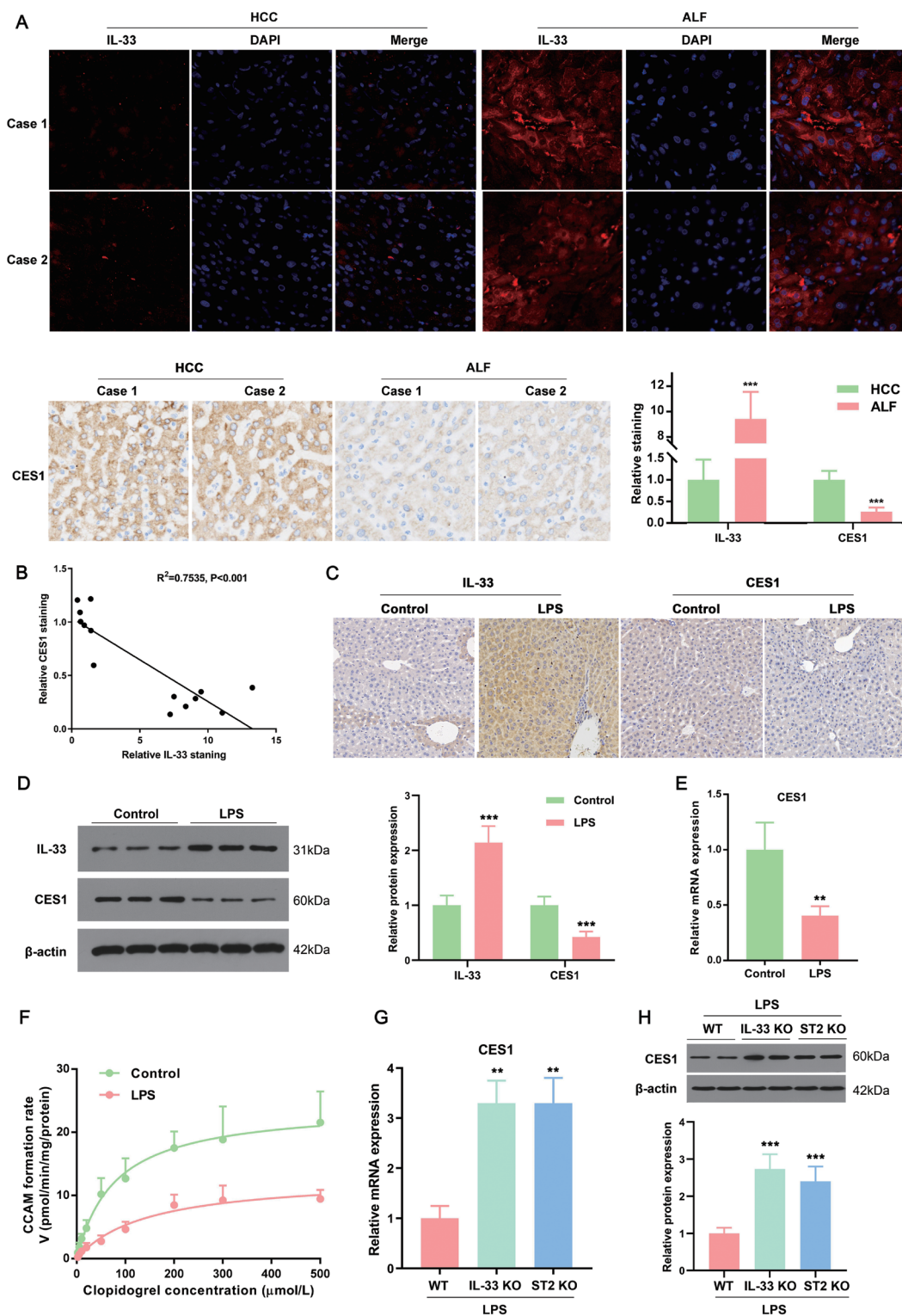


Fig. 1. IL-33 downregulates CES1 in ALF patients and LPS-treated mice. (A) Representative images of IL-33 and CES1 staining in liver biopsy specimens of patients diagnosed with HCC (n=7) or ALF (n=7) (×400). The protein expression levels of IL-33 and CES1 in liver biopsies were quantified by Image-Pro Plus. *** $p<0.001$ vs. HCC group. (B) The linear relationship between IL-33 and CES1 was analyzed. Immunohistochemistry (C) and western blot (D) depict hepatic IL-33 and CES1 expression in control and LPS-treated mice. (E) CES1 mRNA levels in livers of LPS-stimulated mice were determined by qPCR. (F) Hydrolytic activities of CES1 were evaluated by the hydrolysis of clopidogrel to its metabolite CCAM. Hepatic CES1 mRNA (G) and protein levels (H) were determined in WT, IL-33, or ST2 knockout mice stimulated by LPS. Experiments were performed in at least triplicate and the results were presented as mean \pm SD. ** $p<0.01$, *** $p<0.001$ vs. control group or LPS+WT group. IL, interleukin; CES1, carboxylesterase 1; ALF, acute liver failure; HCC, hepatocellular carcinoma; LPS, lipopolysaccharide; SD, standard deviation.

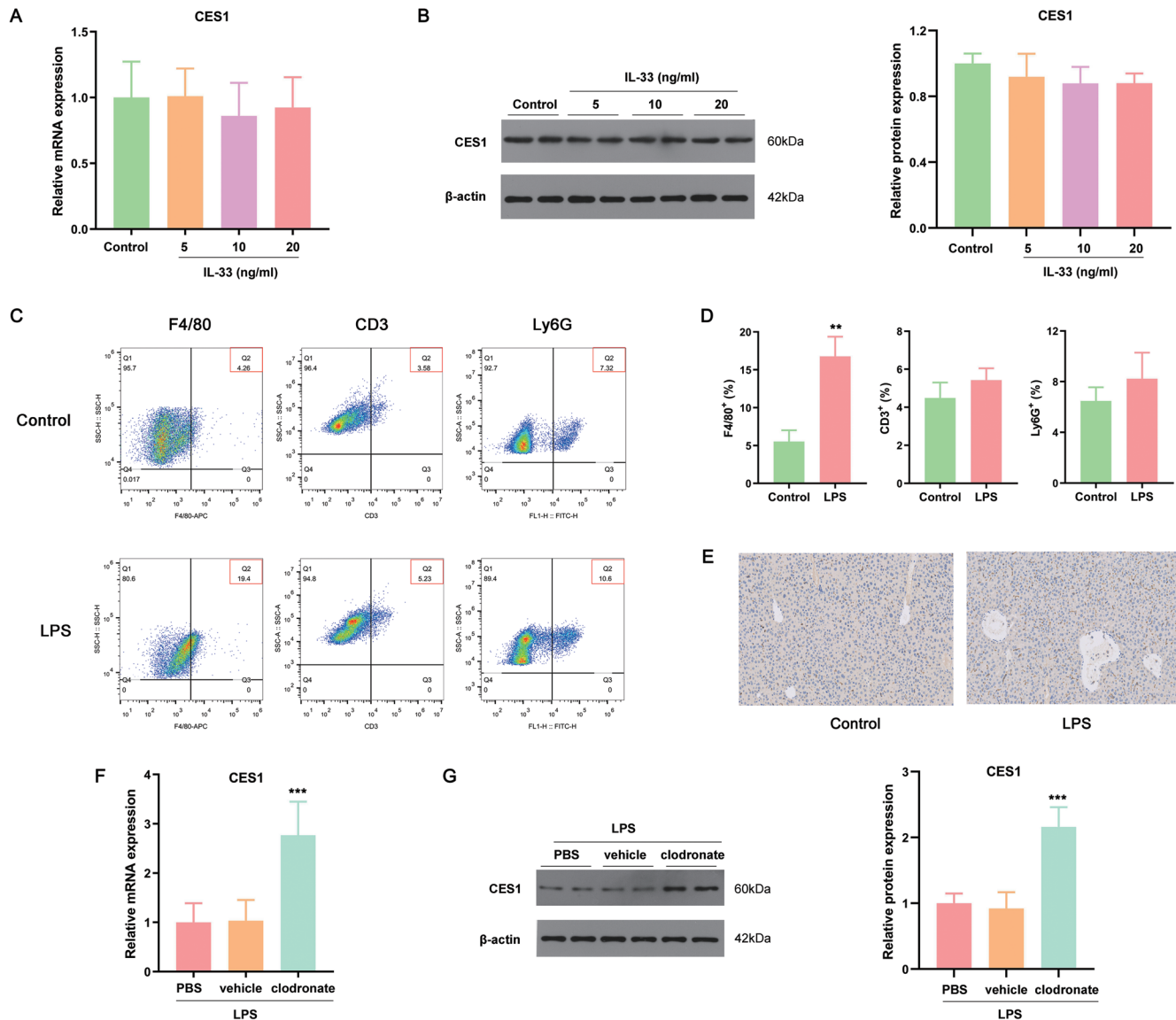


Fig. 2. Macrophage mediates the downregulation of hepatic CES1 by IL-33. CES1 mRNA (A) and protein levels (B) in mouse primary hepatocytes which were treated with vehicle or IL-33 (5, 10 and 20 ng/mL). (C) Flow cytometry was used to determine macrophages (F4/80), T cells (CD3) and neutrophils (Ly6G) in mouse livers and their quantification (D). ** $p < 0.01$ vs. control group. (E) F4/80 in mouse liver tissue was detected by immunohistochemistry ($\times 200$). CES1 mRNA (F) and protein levels (G) in the livers of LPS-induced liver injury in mice which were treated with or without clodronate. *** $p < 0.001$ vs. LPS+vehicle group. Experiments were performed in at least triplicate and the results are means \pm SDs. CES1, carboxylesterase 1; IL, interleukin; LPS, lipopolysaccharide.

identified to be differentially expressed (criteria: $|\log_2(\text{fold change})| > 1$ and $p < 0.05$) in IL-33-MDEs, relative to Con-MDEs, 24 were upregulated and 13 were downregulated (Fig. 4A, B). The top-three most significantly upregulated miRNAs were verified by qRT-PCR (Fig. 4C). One of them, miR-27b-3p, became the focus of our study because it is involved in lipid metabolism²⁴ and has a negatively regulatory influence on cytochrome P450 enzyme expression.^{25,26}

Primary mouse hepatocytes and HepaRG cells that were incubated with IL-33-MDEs had higher expression of miR-27b-3p than PBS-treated or Con-MDE-treated cells (Fig. 4D, E), demonstrating that miR-27b-3p could be delivered to hepatocytes via MDEs. Validation qRT-PCR assays confirmed that primary hepatocytes were transfected with miR-27b-3p mimics, inhibitors, and their negative controls successfully

(Supplementary Fig. 2A). CES1 expression was inhibited by miR-27b-3p mimic and increased by a miR-27b-3p inhibitor (Fig. 4F, G). In an *in vivo* validation experiment, antagomir-negative control, or miR-27b-3p-antagomir was injected into mice. qRT-PCR results confirmed that miR-27b-3p-antagomir injection suppressed miR-27b-3p (Supplementary Fig. 2B). After LPS stimulation, CES1 mRNA and protein levels were recovered in the presence of the miR-27b-3p-antagomir (Fig. 4H, I), suggesting that MDE-packaged miR-27b-3p was essential for IL-33 downregulation of CES1.

miR-27b-3p downregulates CES1 by targeting *Nrf2*

To decipher the target mechanisms underlying the effects of miR-27b-3p, computational analysis with TargetScan, miRDB, RNA22, and miRTarBase databases (Fig. 5A) iden-

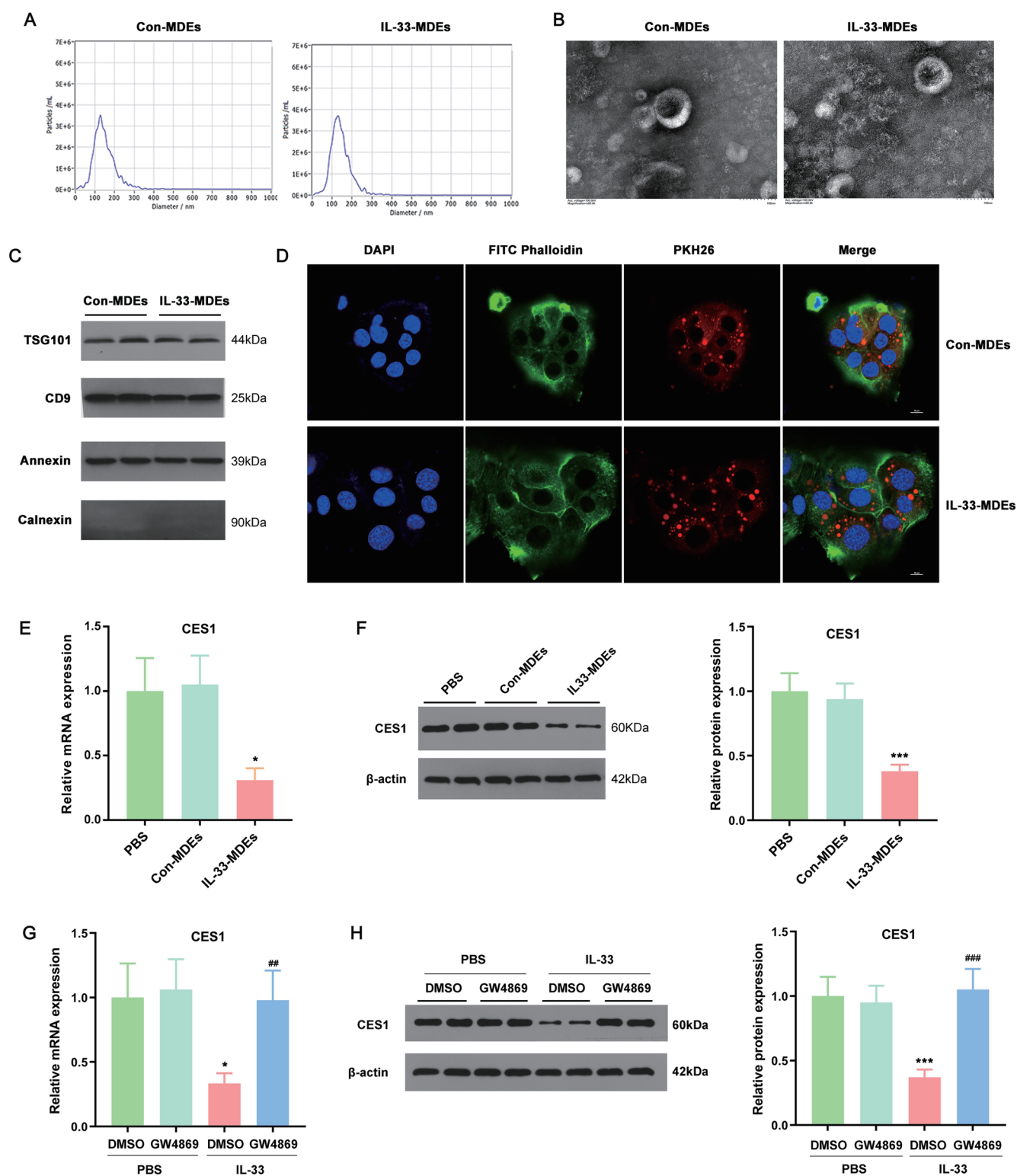


Fig. 3. IL-33 suppresses CES1 through MDEs. (A) Size distribution of the isolated exosomes was analyzed by nanoparticle tracking analysis. (B) Representative transmission electron microscopy images of Con-MDEs and IL-33-MDEs. Scale bar = 100 nm. (C) Indicated proteins TSG101, CD9, Annexin A1, and calnexin were assessed by western blot. (D) Immunofluorescence detection of MDE uptake by hepatocyte. CES1 mRNA (E) and protein levels (F) in hepatocytes treated with PBS, Con-MDEs, or IL-33-MDEs. $^{**}p < 0.01$, $^{***}p < 0.001$ vs. Con-MDEs group. Effects of exosome inhibitor GW4869 on CES1 mRNA (G) and protein levels (H). $^{*}p < 0.05$, $^{***}p < 0.001$ vs. PBS+DMSO group. $^{##}p < 0.01$, $^{###}p < 0.001$ vs. IL-33+DMSO group. Experiments were performed in at least triplicate and the results are means \pm SDs. IL, interleukin; CES1, carboxylesterase 1; MDE, macrophage-derived exosome; PBS, phosphate buffered saline.

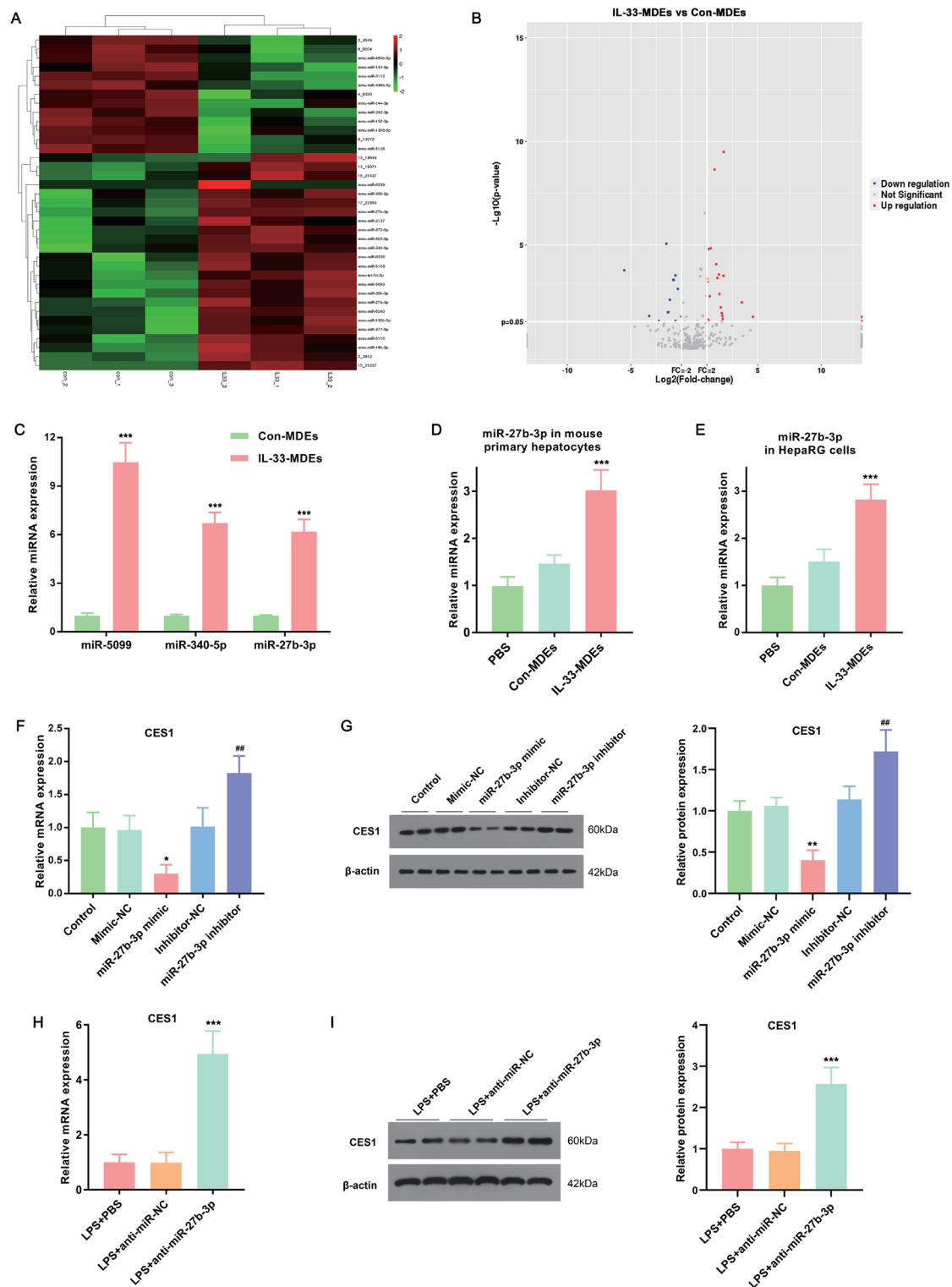


Fig. 4. miR-27b-3p transferred by MDEs mediates the downregulation of CES1 by IL-33. Heatmap (A) and volcano plot (B) of miRNAs differentially expressed between Con-MDEs and IL-33-MDEs. Red: increased expression; green: decreased expression. (C) High expression of miR-5099, miR-340-5p, and miR-27b-3p in IL-33-MDEs was confirmed using qRT-PCR. The expression levels of miR-27b-3p in mouse primary hepatocytes (D) and HepaRG cells (E) treated with PBS, Con-MDEs, or IL-33-MDEs were determined by qRT-PCR. *** $p < 0.001$ vs. Con-MDEs group. CES1 mRNA (F) and protein levels (G) in primary hepatocytes which were transfected with miR-27b-3p mimic, inhibitor, or miR-NC. ** $p < 0.01$, *** $p < 0.001$ vs. mimic-NC group. ## $p < 0.01$ vs. inhibitor-NC group. CES1 mRNA (H) and protein levels (I) in livers of LPS-induced liver injury in mice which were treated with PBS, anti-miR-NC, or anti-miR-27b-3p. *** $p < 0.001$ vs. LPS+anti-miR-NC group. Experiments were performed in at least triplicate and the results are means \pm SDs. miR, micro-RNA; CES1, carboxylesterase 1; MDE, macrophage-derived exosome; SD, standard deviation.

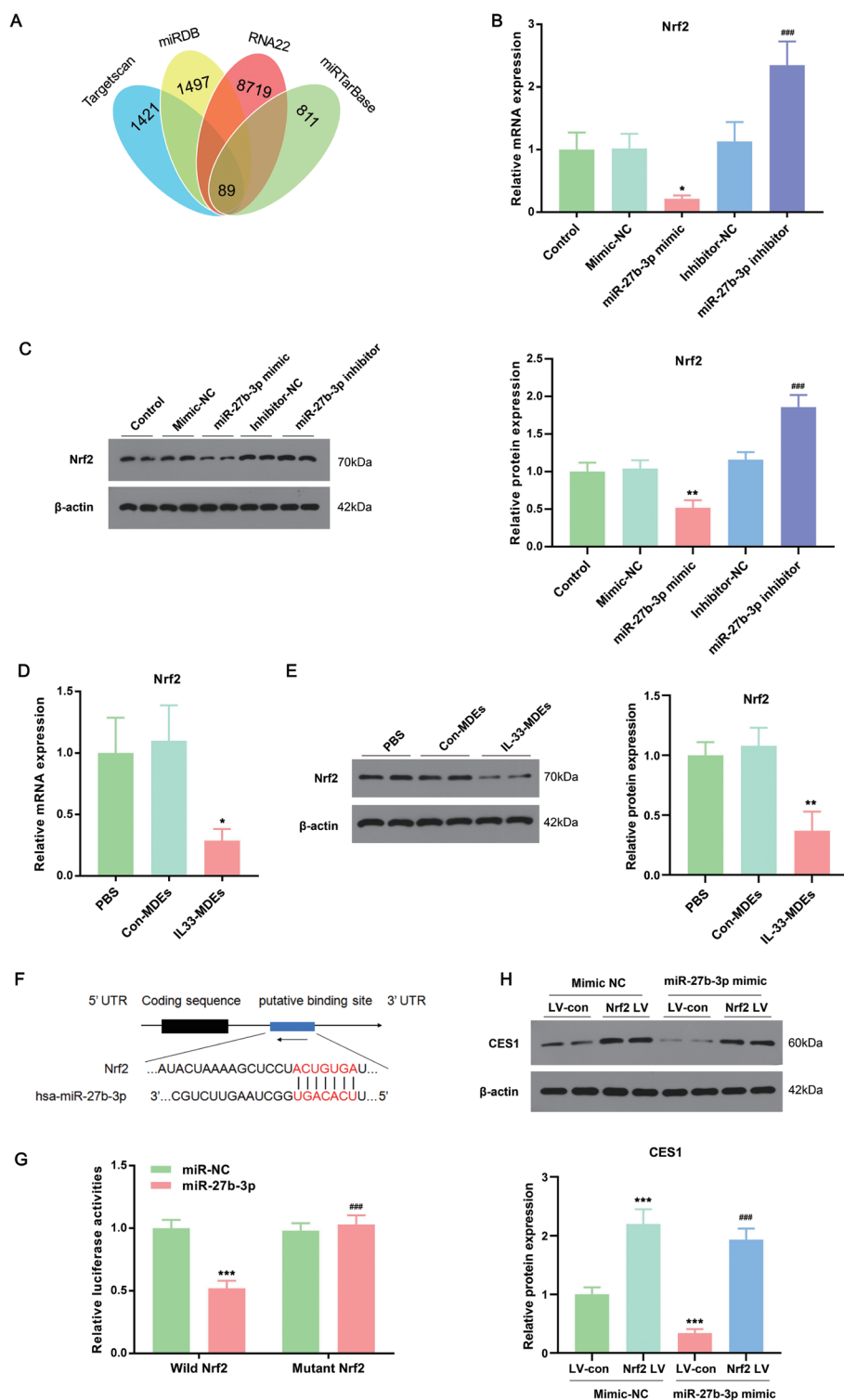


Fig. 5. miR-27b-3p inhibited CES1 by targeting Nrf2. (A) Predicted targets of miR-27b-3p using four independent platforms. Nrf2 mRNA (B) and protein levels (C) in primary hepatocytes which were transfected with miR-27b-3p mimic, inhibitor, or miR-NC. * $p < 0.05$, ** $p < 0.01$ vs. mimic-NC group. *** $p < 0.001$ vs. inhibitor-NC group. Nrf2 mRNA (D) and protein levels (E) in primary hepatocytes which were treated with PBS, con-MDEs, or IL-33-MDEs. * $p < 0.05$, ** $p < 0.01$ vs. Con-MDEs group. (F) Schematic diagram of the WT and mutated-type binding site between miR-27b-3p and Nrf2. (G) Luciferase reporter assay in hepatocytes cotransfected with wild-type or mutant Nrf2 3'UTR reporter gene and miR-27b-3p or miR-NC. *** $p < 0.001$ vs. wild Nrf2+miR-NC group. *** $p < 0.001$ vs. wild Nrf2+miR-27b-3p group. CES1 protein level (H) in HepaRG cells which were infected with lentivirus overexpressing Nrf2 and followed by treatment with miR-27b-3p or miR-NC. *** $p < 0.001$ vs. mimic-NC+LV-con group. *** $p < 0.001$ vs. miR-27b-3p mimic+LV-con group. Experiments were performed in at least triplicate and the results are means \pm SDs. miR, micro-RNA; CES1, carboxylesterase 1; Nrf2, nuclear factor erythroid 2-related factor 2; WT, wild type; SD, standard deviation.

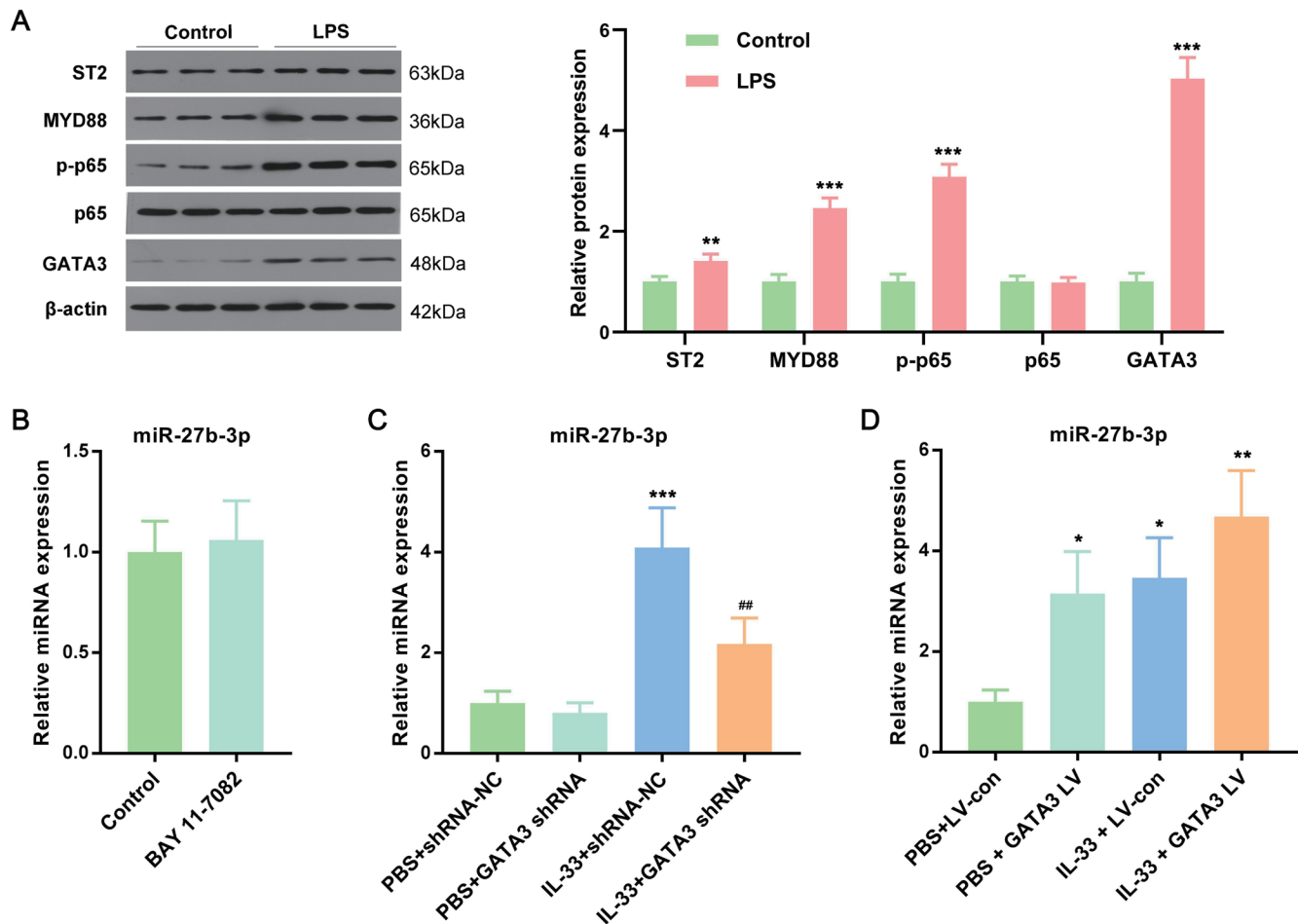


Fig. 6. IL-33 drives the expression of miR-27b-3p through GATA3. (A) The expression of IL-33's downstream in LPS-stimulated RAW264.7 cells. $**p<0.01$, $***p<0.001$ vs. control group. (B) The effect of NF- κ B inhibitors BAY 11-7082 on the miR-27b-3p level in MDEs. MDEs were extracted from PBS or IL-33-treated RAW264.7 cells which were transfected with control, GATA3 shRNA (C) or GATA3-overexpressed lentivirus (D) and then miR-27b-3p level was detected. $*p<0.05$, $**p<0.01$, $***p<0.001$ vs. PBS+shRNA-NC or PBS+LV-con group. $##p<0.01$ vs. IL-33+ shRNA-NC group. IL, interleukin; miR, micro-RNA; MDE, macrophage-derived exosome; PBS, phosphate buffered saline.

tified *Nrf2* (nuclear factor erythroid 2-related factor 2) as a potential target for miR-27b-3p. *Nrf2* mRNA and protein levels were strongly downregulated in hepatocytes treated with miR-27b-3p mimics but could be rescued by a miR-27b-3p inhibitor (Fig. 5B, C). Consistently, compared with Con-MDEs, IL-33-MDEs also decreased hepatocyte expression of *Nrf2* (Fig. 5D, E).

Upon confirming that *Nrf2* held a potential binding site for miR-27b-3p (Fig. 5F), hepatocytes that had been co-transfected with WT or mutated Luc-*Nrf2*-3'UTR together with miR-27b-3p or miR-negative control were subjected to luciferase reporter assays. When nucleotide-substitution mutations were introduced to the predicted binding site of miR-27b-3p in the 3'-UTR of *Nrf2* mRNA, miR-27b-3p lost its ability to affect luciferase activity (Fig. 5G). The results confirm that miR-27b-3p targeted *Nrf2* and inhibited *Nrf2* mRNA expression as well as NRF2 protein expression.

An *Nrf2* rescue assay in which *Nrf2*-transfected HepaRG cells (Supplementary Fig. 3) were treated with miR-27b-3p mimic or a negative control mimic confirmed that exosomal miR-27b-3p effects were mediated by repression of *Nrf2* in hepatocytes. Western blot analysis showed that *Nrf2* overexpression reversed miR-27b-3p effects on CES1 downregulation completely (Fig. 5H). The results suggested that an inhibitory effect of miR-27b-3p contributes to targeted inhibition of *Nrf2*.

tion completely (Fig. 5H). The results suggested that an inhibitory effect of miR-27b-3p contributes to targeted inhibition of *Nrf2*.

GATA3 drives expression of miR-27b-3p

We next investigated the molecular mechanism on how IL-33-ST2 signaling induced miR-27b-3p. LPS treatment of RAW264.7 cells increased ST2 and MyD88 levels, as well as levels of NF- κ B and GATA3, each of which is a molecule in a signaling pathway downstream of MyD88 (Fig. 6A). No significant effect on miR-27b-3p levels in MDEs was observed when RAW264.7 cells were exposed to the NF- κ B inhibitor BAY 11-7082 (Fig. 6B and Supplementary Fig. 4A). Conversely, *Gata3* silencing reduced miR-27b-3p content in MDEs markedly (Fig. 6C), and lentivirus system-induced *Gata3* overexpression (Supplementary Fig. 4B) increased the miR-27b-3p content in MDEs strongly (Fig. 6D).

In summary, these results suggest that IL-33 inhibits the expression of CES1 upon liver injury. Mechanistically, the IL-33-ST2-GATA3 axis increases miR-27b-3p content in MDEs, which can be internalized by hepatocytes and thus then reduces CES1 expression by inhibiting its target gene *Nrf2* (Fig. 7).

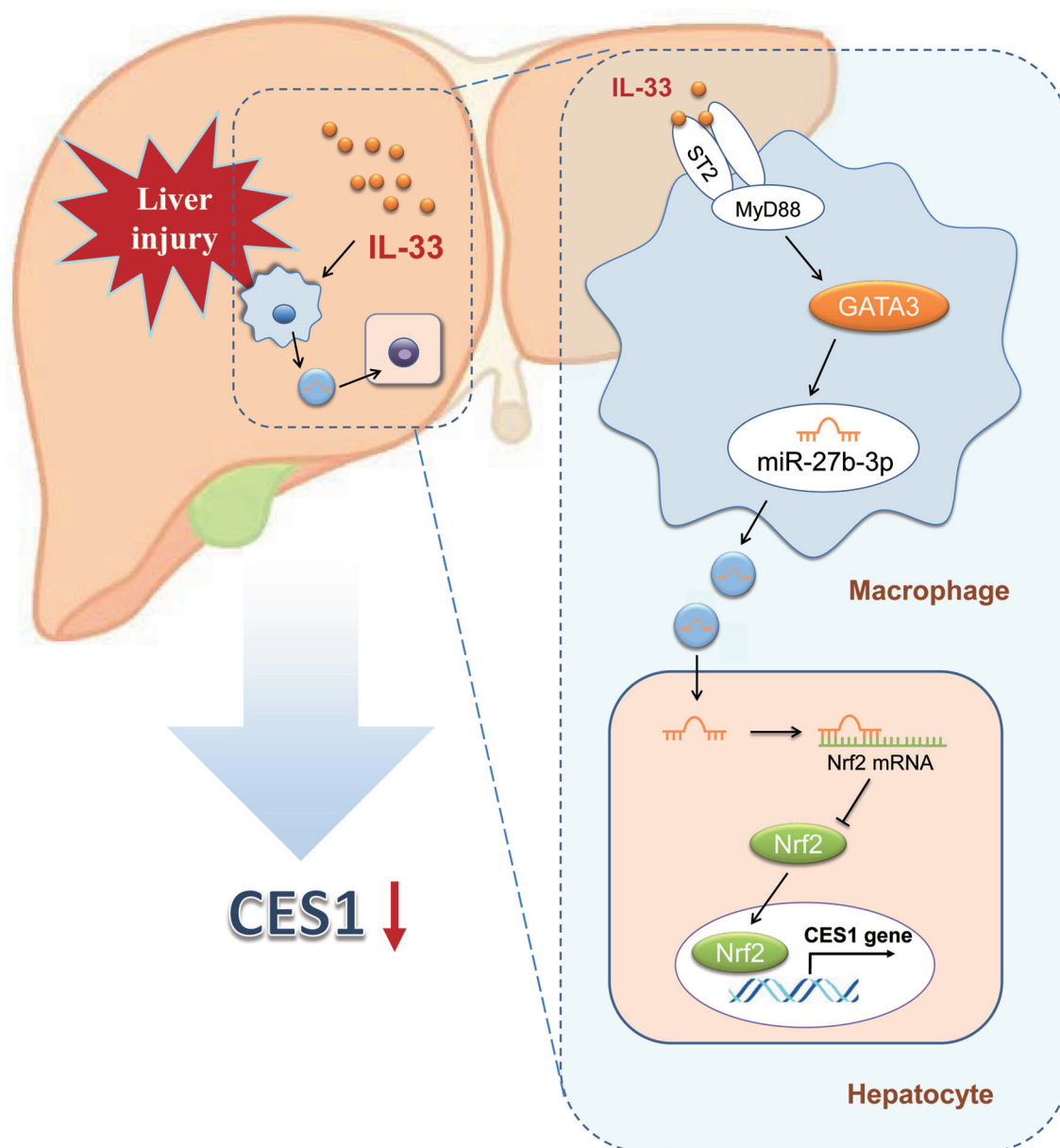


Fig. 7. Summary of the mechanism by which IL-33 suppresses CES1 in liver injury. CES1, carboxylesterase 1; IL, interleukin.

Discussion

In this study, we identified IL-33 as a potent CES1 suppressor following liver injury and found that the suppression occurred in an ST2-dependent manner. We found that IL-33, a dominant regulator in liver injury,^{13–16} was elevated while CES1 was reduced in both LPS- and APAP-treated mice, as well as in pathological specimens from patients, in line with previous reports.^{7,13,14,16} Using a loss-of-function approach, we demonstrated that IL-33 was necessary for the downregulation of CES1 in liver injury. Further, the inhibition of CES1 was abolished in ST2 KO mice. These data confirm a potent role of IL-33 in CES1 downregulation. To our knowledge, this study is the first to identify IL-33 as a key regulator of CES1 in liver injury.

In our first attempt to explore the underlying mechanism

by which IL-33 suppressed CES1, primary hepatocytes, the source cells of CES1, were treated with IL-33. However, we did not observe inhibition of CES1, perhaps due to weak ST2 expression in the hepatocytes.²⁷ Hence, we examined the cells with high ST2 expression in the liver. Flow cytometry and immunohistochemical results suggested that macrophages may be responsible for IL-33 effects on CES1. This finding was further supported by the restoration of CES1 in macrophage-depleted mice. Liver-resident macrophages, known as Kupffer cells, account for 15% of total liver cells. Previous studies in alcoholic and APAP-induced liver injury have shown that macrophages act as IL-33 target cells to exacerbate liver damage.^{14,28} Consistent with these studies, we verified that liver macrophages were IL-33 responsive.

Recent studies have suggested that the hepatic system may depend on intercellular communication that occurs via

exosomes.²⁹ Here, we found that MDEs could be taken up by hepatocytes and then mediate downregulation of CES1 by IL-33. Furthermore, inhibition of exosome release rescued CES1 expression, suggesting that MDEs are indispensable for IL-33's role in CES1 regulation. Exosomes can transfer a variety of cargo into recipient cells, including proteins, lipids, DNAs, mRNAs, and miRs. Because exosome-carried miRs play a particularly important role in liver disorders,²⁹ we used miR-Seq to analyze miR profiles in IL-33-MDEs. We found that miR-27b-3p levels were significantly greater in IL-33-MDEs than in Con-MDEs; and miR-27b-3p involvement was confirmed *in vivo* and *in vitro*. Subsequently, we determined that miR-27b-3p inhibited CES1 by targeting *Nrf2*.

miR-27b has been identified as a regulatory hub of lipid metabolism in the liver, and its overexpression results in lipid accumulation.^{30,31} Hepatic CES1 has been demonstrated to hydrolyze triglycerides and to stimulate fatty acid oxidation, thereby playing an essential role in lipid homeostasis.³² Our study revealed a novel potential mechanism, namely CES1 suppression, by which miR-27b may exert its effects, which previously have been shown to include lipid metabolism impairment via inhibition of adipogenesis.³³

IL-33 is a dual-function protein, acting as an intracellular nuclear factor as well as a potent extracellular cytokine.²² The absence of IL-33 induced modulation on CES1 in ST2-deficient mice suggested that IL-33 may act through the extracellular ST2 pathway rather than as a nuclear factor. After binding of IL-33 and ST2 in the canonical IL-33-ST2 signaling pathway, the complex recruits intracellular signaling molecules, including MyD88/IL-1 receptor-associated kinase/TRAF6, and activates NF- κ B.²² Recently, GATA3 was identified as an IL-33-responsive transcriptional hub in macrophages.³⁴ Here, gain- and loss-of-function experimental results suggested that IL-33 induced miR-27b-3p effects were mediated through GATA3, rather than NF- κ B. However, the underlying process by which GATA3 promotes miR-27b-3p remains to be elucidated.

Conclusions

Our findings demonstrated that IL-33 acts to downregulate CES1 in injured liver. Mechanistically, we found that increased extracellular IL-33 in liver injury triggered IL-33-ST2-GATA3 signaling, and then stimulated miR-27b-3p expression in hepatic macrophages. Exosome transfer of miR-27b-3p to hepatocytes inhibited its target gene, *Nrf2*, thereby suppressing CES1 expression. Strong inhibition of CES1 will slow the hydrolysis of CES1 substrates, including drugs and lipids, which in turn, impacts the pharmacokinetic and toxicological profiles of these substances. The identification of this intercellular communication mechanism strengthens our understanding of CES1 downregulation in acute liver injury and may aid in the future development of biomedical applications of CES1.

Acknowledgments

We thank Medjaden Inc. for scientific editing of this manuscript.

Funding

This work was supported by the National Natural Science Foundation of China (81670521 and 81803798).

Conflict of interest

The authors have no conflict of interests related to this publication.

Author contributions

Designed the research (PG, ML, JL, CZ), participated part of the experiments and wrote the manuscript (PG), carried out the experiments (ML, DX, XW, YX, YZ, GL), performed data analysis and revised the manuscript (JL, XG, CZ). All authors have read and approved the final manuscript.

Ethical statement

All experimental procedures were performed in accordance with the Declaration of Helsinki of the World Medical Association and were approved by the Medical Ethics Committee of Tongji Hospital (no: TJ-IRB20210961). All mice were bred and maintained under specific pathogen-free conditions and studied in compliance with the Animal Care and Use Committee guidelines of Tongji Hospital, Tongji Medical College, HUST.

Data sharing statement

No additional data are available.

References

- [1] Wang D, Zou L, Jin Q, Hou J, Ge G, Yang L. Human carboxylesterases: a comprehensive review. *Acta Pharm Sin B* 2018;8(5):699–712. doi:10.1016/j.apsb.2018.05.005, PMID:30245959.
- [2] Her L, Zhu HJ. Carboxylesterase 1 and Precision Pharmacotherapy: Pharmacogenetics and Nongenetic Regulators. *Drug Metab Dispos* 2020; 48(3):230–244. doi:10.1124/dmd.119.089680, PMID:31871135.
- [3] Metz MZ, Gutova M, Lacey SF, Abramyan Y, Vo T, Gilchrist M, *et al*. Neural stem cell-mediated delivery of irinotecan-activating carboxylesterases to glioma: implications for clinical use. *Stem Cells Transl Med* 2013; 2(12):983–992. doi:10.5966/sctm.2012-0177, PMID:24167321.
- [4] Quiroga AD, Li L, Trotschmuller M, Nelson R, Proctor SD, Kofeler H, *et al*. Deficiency of carboxylesterase 1/esterase-x results in obesity, hepatic steatosis, and hyperlipidemia. *Hepatology* 2012;56(6):2188–2198. doi:10.1002/hep.25961, PMID:22806626.
- [5] Capece D, D'Andrea D, Begalli F, Goracci L, Tornatore L, Alexander JL, *et al*. Enhanced triacylglycerol catabolism by carboxylesterase 1 promotes aggressive colorectal carcinoma. *J Clin Invest* 2021;131(11):e137845. doi:10.1172/JCI137845, PMID:33878036.
- [6] Braeuning A, Schwarz M. Regulation of expression of drug-metabolizing enzymes by oncogenic signaling pathways in liver tumors: a review. *Acta Pharm Sin B* 2020;10(1):113–122. doi:10.1016/j.apsb.2019.06.013, PMID:31993310.
- [7] Zhang C, Xu Y, Gao P, Lu J, Li X, Liu D. Down-regulation of carboxylesterases 1 and 2 plays an important role in prodrug metabolism in immunological liver injury rats. *Int Immunopharmacol* 2015;24(2):153–158. doi:10.1016/j.intimp.2014.12.003, PMID:25499727.
- [8] Chalasani N, Gorski JC, Patel NH, Hall SD, Galinsky RE. Hepatic and intestinal cytochrome P450 3A activity in cirrhosis: effects of transjugular intrahepatic portosystemic shunts. *Hepatology* 2001;34(6):1103–1108. doi:10.1053/jhep.2001.29306, PMID:11731998.
- [9] Robinson MW, Harmon C, O'Farrelly C. Liver immunology and its role in inflammation and homeostasis. *Cell Mol Immunol* 2016;13(3):267–276. doi:10.1038/cmi.2016.3, PMID:27063467.
- [10] Dunvald AD, Jarvinen E, Mortensen C, Stage TB. Clinical and Molecular Perspectives on Inflammation-Mediated Regulation of Drug Metabolism and Transport. *Clin Pharmacol Ther* 2021;112(2):277–290. doi:10.1002/cpt.2432, PMID:34605009.
- [11] Li M, Lan L, Zhang S, Xu Y, He W, Xiang D, *et al*. IL-6 downregulates hepatic carboxylesterases via NF- κ B activation in dextran sulfate sodium-induced colitis. *Int Immunopharmacol* 2021;99:107920. doi:10.1016/j.intimp.2021.107920, PMID:34217990.
- [12] Kreutz RP. IL-1R (Interleukin-1 Receptor) Signaling and Attenuated Hepatic CYP (Cytochrome P450) 2C Expression: Explanation for Higher Rate of Clopidogrel Resistance in Patients With Diabetes Mellitus? *Arterioscler Thromb Vasc Biol* 2020;40(6):1429–1431. doi:10.1161/ATVBAHA.120.314446, PMID:32459538.
- [13] Xu L, Yang Y, Wen Y, Jeong JM, Emontzophl C, Atkins CL, *et al*. Hepatic recruitment of eosinophils and their protective function during acute liver injury. *J Hepatol* 2022;77(2):344–352. doi:10.1016/j.jhep.2022.02.024, PMID:35259470.
- [14] Wang M, Shen G, Xu L, Liu X, Brown JM, Feng D, *et al*. IL-1 receptor like 1 protects against alcoholic liver injury by limiting NF- κ B activation in hepatic macrophages. *J Hepatol* 2018;68(1):109–117. doi:10.1016/j.jhep.2017.08.023, PMID:28870670.
- [15] Liang Y, Yi P, Yuan DMK, Jie Z, Kwota Z, Soong L, *et al*. IL-33 induces immunosuppressive neutrophils via a type 2 innate lymphoid cell/IL13/STAT6 axis and protects the liver against injury in LCMV infection-induced viral hepatitis. *Cell Mol Immunol* 2019;16(2):126–137. doi:10.1038/cmi.

- 2017;147, PMID:29400707.
- [16] Yazdani HO, Chen HW, Tohme S, Tai S, van der Windt DJ, Loughran P, *et al*. IL-33 exacerbates liver sterile inflammation by amplifying neutrophil extracellular trap formation. *J Hepatol* 2017;68(1):130–139. doi:10.1016/j.jhep.2017.09.010, PMID:28943296.
- [17] Shao L, Xiong X, Zhang Y, Miao H, Ren Y, Tang X, *et al*. IL-22 ameliorates LPS-induced acute liver injury by autophagy activation through ATF4-ATG7 signaling. *Cell Death Dis* 2020;11(11):970. doi:10.1038/s41419-020-03176-4, PMID:33177520.
- [18] Groeneveld D, Cline-Fedewa H, Baker KS, Williams KJ, Roth RA, Mittermeier K, *et al*. Von Willebrand factor delays liver repair after acetaminophen-induced acute liver injury in mice. *J Hepatol* 2020;72(1):146–155. doi:10.1016/j.jhep.2019.09.030, PMID:31606553.
- [19] Zhang Y, Xue W, Zhang W, Yuan Y, Zhu X, Wang Q, *et al*. Histone methyltransferase G9a protects against acute liver injury through GSTP1. *Cell Death Differ* 2020;27(4):1243–1258. doi:10.1038/s41418-019-0412-8, PMID:31515511.
- [20] Marques-Garcia F, Isidoro-Garcia M. Protocols for Exosome Isolation and RNA Profiling. *Methods Mol Biol* 2016;1434:153–167. doi:10.1007/978-1-4939-3652-6_11, PMID:27300537.
- [21] Mello T, Nakatsuka A, Fears S, Davis W, Tsukamoto H, Bosron WF, *et al*. Expression of carboxylesterase and lipase genes in rat liver cell-types. *Biochem Biophys Res Commun* 2008;374(3):460–464. doi:10.1016/j.bbrc.2008.07.024, PMID:18639528.
- [22] Cayrol C, Girard JP. Interleukin-33 (IL-33): A nuclear cytokine from the IL-1 family. *Immunol Rev* 2018;281(1):154–168. doi:10.1111/immr.12619, PMID:29247993.
- [23] Heymann F, Tacke F. Immunology in the liver—from homeostasis to disease. *Nat Rev Gastroenterol Hepatol* 2016;13(2):88–110. doi:10.1038/nrgastro.2015.200, PMID:26758786.
- [24] Castano C, Kalko S, Novials A, Parrizas M. Obesity-associated exosomal miRNAs modulate glucose and lipid metabolism in mice. *Proc Natl Acad Sci USA* 2018;115(48):12158–12163. doi:10.1073/pnas.1808855115, PMID:30429322.
- [25] Li X, Tian Y, Tu MJ, Ho PY, Batra N, Yu AM. Bioengineered miR-27b-3p and miR-328-3p modulate drug metabolism and disposition via the regulation of target ADME gene expression. *Acta Pharm Sin B* 2019;9(3):639–647. doi:10.1016/j.apsb.2018.12.002, PMID:31193825.
- [26] Mu W, Hu C, Zhang H, Qu Z, Cen J, Qiu Z, *et al*. miR-27b synergizes with anticancer drugs via p53 activation and CYP1B1 suppression. *Cell Res* 2015;25(4):477–495. doi:10.1038/cr.2015.23, PMID:25698578.
- [27] Antunes MM, Araujo AM, Diniz AB, Pereira RVS, Alvarenga DM, David BA, *et al*. IL-33 signalling in liver immune cells enhances drug-induced liver injury and inflammation. *Inflamm Res* 2018;67(1):77–88. doi:10.1007/s00011-017-1098-3, PMID:29032512.
- [28] Wang Z, Wu L, Pan B, Chen Y, Zhang T, Tang N. Interleukin 33 mediates hepatocyte autophagy and innate immune response in the early phase of acetaminophen-induced acute liver injury. *Toxicology* 2021;456:152788. doi:10.1016/j.tox.2021.152788, PMID:33887374.
- [29] Sato K, Meng F, Glaser S, Alpini G. Exosomes in liver pathology. *J Hepatol* 2016;65(1):213–221. doi:10.1016/j.jhep.2016.03.004, PMID:26988731.
- [30] Vickers KC, Shoucri BM, Levin MG, Wu H, Pearson DS, Osei-Hwedie D, *et al*. MicroRNA-27b is a regulatory hub in lipid metabolism and is altered in dyslipidemia. *Hepatology* 2013;57(2):533–542. doi:10.1002/hep.25846, PMID:22777896.
- [31] Singaravelu R, Chen R, Lyn RK, Jones DM, O'Hara S, Rouleau Y, *et al*. Hepatitis C virus induced up-regulation of microRNA-27: a novel mechanism for hepatic steatosis. *Hepatology* 2014;59(1):98–108. doi:10.1002/hep.26634, PMID:23897856.
- [32] Xu J, Li Y, Chen WD, Xu Y, Yin L, Ge X, *et al*. Hepatic carboxylesterase 1 is essential for both normal and farnesoid X receptor-controlled lipid homeostasis. *Hepatology* 2014;59(5):1761–1771. doi:10.1002/hep.26714, PMID:24038130.
- [33] Kong X, Yu J, Bi J, Qi H, Di W, Wu L, *et al*. Glucocorticoids transcriptionally regulate miR-27b expression promoting body fat accumulation via suppressing the browning of white adipose tissue. *Diabetes* 2015;64(2):393–404. doi:10.2337/db14-0395, PMID:25187367.
- [34] Faas M, Ipseiz N, Ackermann J, Culemann S, Gruneboom A, Schroder F, *et al*. IL-33-induced metabolic reprogramming controls the differentiation of alternatively activated macrophages and the resolution of inflammation. *Immunity* 2021;54(11):2531–2546.e2535. doi:10.1016/j.immuni.2021.09.010, PMID:34644537.